L16 orthogonal design synthesis of NASICON-type Li1.4Al0.4Ti1.6(PO4)3 solid electrolyte by Pechini method for process optimization

Mohammad Reza Ghaania, Pirooz Marashi*[a]

[1] *Department of Mining and Metallurgical Engineering, Amirkabir University of Technology, Tehran, Iran P. O. Box 15875-4413*

Abstract

Na super ionic conductive (NASICON) materials are ceramics with three-dimensional scaffolds. In this study, $Li_{1.4}Al_{0.4}Ti_{1.6}(PO_4)_3$ with NASICON structure was synthesized by Pechini method. As a result, a sample having a total conduction of 1.18×10^{-3} S cm^{-1} was attained. In addition, various parameters were studied to obtain high value of conductivity, by optimizing the process. The optimization was made using L16 Taguchi based orthogonal array, followed by ANOM, ANOVA and stepwise regression. As a result, the optimum synthesis parameters can be obtained, while pH of the solution was adjusted to 7. The ratio between the concentration of citric acid to metal ions and ethylene glycol concentration stuck to 1 and 2.5, respectively. The best heat treatment can be carried out with a combination of pyrolysis at 600 ºC and sintering at 1000 ºC. Keywords: L16 orthogonal array; NASICON; Pechini; Ionic conductivity; ANOM; Stepwise regression; Electrochemical impedance spectroscopy; LATP; Peroxotitanium.

1. Introduction

During the last decade solid lithium ion conductors have found widespread applications in areas such as high-energy lithium ion batteries [1-3], electrochemical sensors [4-6] and supercapacitors [7] due to their high ionic conductivity and relatively high chemical stability [8, 9]. Sodium supersonic conductor (NASICON), with a 3D framework structure, is compound as a major fast ionic conduction compound.

Various methods for the synthesis of this ceramic compound such as sol-gel [10-12], solid state [13-15] and melt quenching [16-18] process have been used. Sol-gel has several advantages, such as: much lower processing temperatures, a high homogeneity of the resulting structures, the possibility of obtaining pure phase of multi-component metal oxides [19], low manufacturing cost, simple stoichiometry control, and fast deposition rate [20]. Generally Alkoxides as organometallic reagents [21, 22] or soluble metallic salts (used in Pechini method) [23-25], have applied for sol-gel

synthesis of this structure. However, the main disadvantage of alkoxides is their extreme sensitivity to moisture and a high reactivity toward hydrolysis, which affect the hydroxylation process [26].

Pechini process consists of two combined stages; a process of forming metal complexes and in situ polymerization of organic compounds [27]. In general, hydroxycarboxylic acids are used to form stable metal complexes. The polyesterification of metal complexes is reached using a polyhydroxy alcohol and finally a rigid organic polymer is produced. Immobilization of metal complexes in this rigid polymeric network ensures the compositional homogeneity. Thereafter, the polymeric resin is calcinated and a pure phase of multi-component metal oxides is attained [28].

Xu et al. (2007) demonstrated that using citric acid-assisted sol–gel process, it is possible to obtain well crystallized glass-ceramics of $Li_{1.4}Al_{0.4}Ti_{1.6}(PO_4)_3$ at a much lower temperature in a shorter synthesis time compared to the conventional solid-state method. They reported that the optimized conditions for citrate-based manufacturing process are: the molar ratio of [citric acid + ethylene glycol]/[Li^{+}+Al^{3+}+Ti^{4+}] = 4 and pH = 7 [19]. Additionally, Mariappan et al. (2006) successfully prepared NASICOnN-type nanostructured material by a Pechini like polymerizable complex method. The optimum conditions of the synthesis process were [ethylene glycol]/[citric acid] = 1 with calcination of the powder precursor in the temperature range of 650 to 1050°C [26]. However, a review of the literature shows that there are few reports on the effect of important parameters of Pechini synthesis on the electrical property of NASICON materials.

Moreover, the investigation of relevant factors in synthesis processes has traditionally been carried out by taking into account the factors in isolation and the ‘one factor at a time’ methodology which is not considered efficient design strategy. An appropriate approach is to apply one of the proposed experimental design methods such as factorial, response surface methodology, Taguchi and etc. [29-32]. These techniques are able to simultaneously view on a number of factors at different levels; however, such approach is hardly observed for the synthesis purposes. While in a synthesis process,

such as sol-gel, there is a complex chemistry and there are several series of efficient parameters. Therefore, to achieve the desired properties as a result of optimization in synthesis conditions, the use of experimental design is critical.

The aim of this study is investigating the effect of some important parameters including citric acid to metallic ions ratio, pH, citric acid to ethylene glycol ratio, calcination and sintering temperatures on the Pechini synthesis of NASICON type ceramic employing design of experiments. In addition, the optimum synthesis conditions and a mathematical model for the conductivity value as a function of synthesis parameters are provided. Electrochemical impedance spectroscopy and X-ray diffraction analysis are used to characterize the properties of the final product obtained.

2. Experimental

Li_2CO_3 (Sigma-Aldrich), Ti powder, $Al(NO_3)_3.9H_2O$ and $NH_4H_2PO_4$ (Merck) were used in the synthesis of $Li_{1.4}Al_{0.4}Ti_{1.6}(PO_4)_3$ powder (LATP). In the early stage, peroxotitanium solution was prepared by dissolving Ti metal powder (Sigma-Aldrich, 99.98%) in hydrogen peroxide (Merck, 30%) and ammonia (Merck, 25%). To prevent the precipitation of Titanium hydroxide and achieving a stable, transparent sol, citric acid is added. [33]. Further, a solution of lithium carbonate, ammonium dihydrogen phosphate and ethylene glycol (EG) (Sigma-Aldrich, >99%) was added to make the final solution. The esterification reaction at 80 °C after 3 hours transfers the sol into a solid, rigid gel. The final product will be prepared by two steps of heat treatment on the formed gel. Both calcination and sintering procedures were carried out using an aluminum crucible in a Carbolite tube furnace (air atmosphere) with a heating rate of 2 °C min^{-1} up to the final temperatures, the samples were 2 h. The synthesis procedure is illustrated in Figure 1 .

Phase analysis was performed by X-ray diffraction, XRD, (Bruker D8) using Cu-Kα radiation (λ=1.5419Å) over the 2θ range of 10°-70° in 0.02° steps. To measure the ion conductivity, cylindrical disks with 13mm diameter and 2mm thickness were prepared and silver ink was used to

make the blocking electrodes at both sides of the pellets. The complex impedance measurements were performed using Autolab impedance analyzer over the frequency range of $1–10^6$ Hz at 50 points.

According to previous studies pH, CA/M and CA/EG ratios of the prepared sol, as well as calcining and sintering temperatures were selected as the most effective parameters in our selected synthesis method [19, 26, 34]. Where M is the total moles of metallic ions present in the solution .

The L16 orthogonal array of Taguchi method [35] was used in order to optimize the results and find out the most important parameters. Then ANOVA was used to determine the effectiveness of each parameter on the conduction through grains and grain boundaries. Regression analysis is carried out

to find the optimum synthesis conditions by using stepwise backward elimination in order to obtain maximum ionic conductivity .

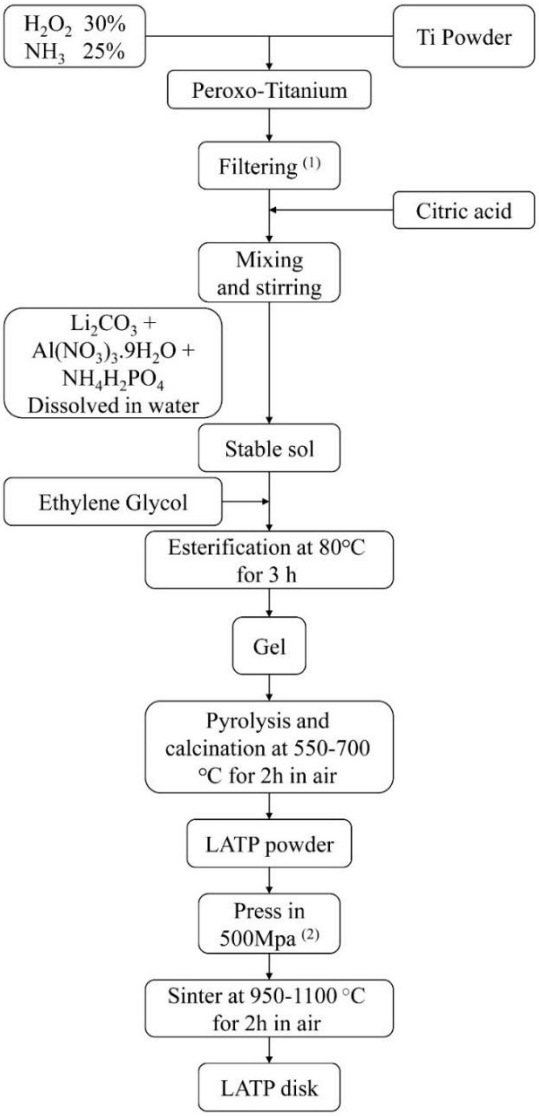

Figure 1- The Pechini synthesis of NASICON type structure. (1) The filtering step is to remove unreacted titanium powders from the solution. Afterward the citric acid has to be added immediately to stop titanium to react with water. (2) No additional binder was used for the disk preparation.

To define each factor the L16 array must be evaluated in four levels (Table 1) in a range that is selected based on the earlier literature [19, 26]. L16 proposes 16 different runs with different combinations of each selected factors (Table 2).

Table 1- The defined values for each level of studied parameters. M is the total moles of metallic ions present in the solution.

pH	CA/M	CA/EG	$T_{cal.}$(°C)	$T_{sin.}$(°C)

5	0.75	0.5	550	1100
6	1	1	600	950
7	1.5	2	650	1000
8	2	2.5	700	1050

Table 2- The proposed runs based on the L16 orthogonal design

Run	pH	CA/M	CA/EG	$T_{cal.}$(°C)	$T_{sin.}$(°C)
1	5	0.75	1	550	1100
2	5	1	1.5	600	950
3	5	0.5	2	650	1000
4	5	2	2.5	700	1050
5	6	0.75	1.5	650	1050
6	6	1	1	700	1000
7	6	0.5	2.5	550	950
8	6	2	2	600	1100
9	7	0.75	2	700	950
10	7	1	2.5	650	1100
11	7	0.5	1	600	1050
12	7	2	1.5	550	1000
13	8	0.75	2.5	600	1000
14	8	1	2	550	1050
15	8	0.5	1.5	700	1100
16	8	2	1	650	950

3. Results and Discussion

3.1. Electrochemical Impedance Spectroscopy Studies

A typical recorded Nyquist diagram for the 16 samples is illustrated in Figure 2. The Ri values of each tested sample, were determined from the simulated Nyquist plots as shown in Figure 2. The equivalent circuit for the assembly consists of pure resistance (R0 and R1) and a constant phase element (CPEe and CPE1). There is no doubt that R0 + R1 is the total resistance (Rtotal) of the sample. However, there are some arguments about the determination of grain and grain-boundary resistance (Rb and Rgb). Several reports directly attributed R0 to the resistance of ion migration in the mass of LATP; while, R1 was attributed to the grain boundary of the LATP plate [36-39].

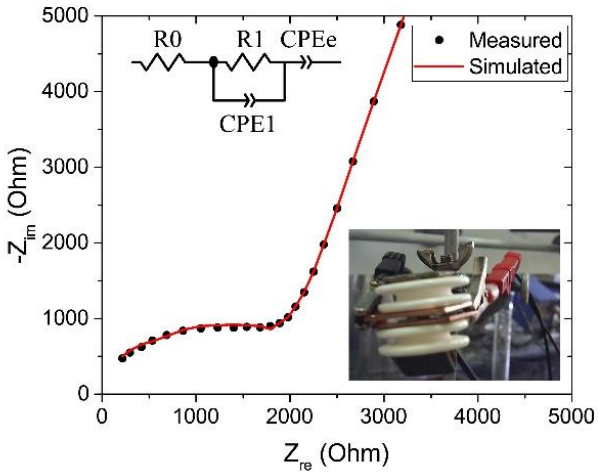

Figure 2- A typical recorded Nyquist plot along with the simulated curve using the presented equivalent circuit. R0 and R1 represents the resistance of grain and the grain boundary respectively. A handmade setup was used to measure the impedance in solid state m mode. Silver ink was applied on both sides of the prepared disk to have electrodes with a good contact. Two cupper plates were delivered the electricity from the instrument connections to the coated electrodes while a same amount of pressure was applied to tighten the cell. 50 logarithmically spaced points were recorded for each sample in the frequency range of 1–106 Hz at room temperature.

To compare the data from different samples, the conductivity value of each sample was calculated using the following equation. As a result, the final value was corrected with regards to the dimensional differences of the samples.

$$\sigma_i = \frac{4t}{\pi D^2 R_i}$$

where σ_i and R_i are the conductivity and the resistance of component i, and t and D are thickness and diameter of the analyzed disk, respectively. The values of the total conductivity (σ_{total}), the conductivity of the grains (σ_b) and the conductivity of the grain boundaries (σ_{gb}) are listed in Table 3.

Run	σ_{total} (S.cm^{-1})	σ_b (S.cm^{-1})	σ_{gb} (S.cm^{-1})
1	2.5×10^{-5}	8.3×10^{-3}	2.6×10^{-5}
2	3.5×10^{-5}	3.9×10^{-3}	3.6×10^{-5}
3	7.0×10^{-5}	4.4×10^{-2}	7.0×10^{-5}
4	9.6×10^{-6}	4.0×10^{-3}	9.6×10^{-6}
5	4.3×10^{-5}	5.5×10^{-3}	4.3×10^{-5}
6	5.5×10^{-5}	1.9×10^{-3}	5.6×10^{-5}

7	4.7×10^{-5}	2.7×10^{-2}	4.9×10^{-5}
8	3.9×10^{-5}	8.0×10^{-3}	3.9×10^{-5}
9	1.3×10^{-5}	4.2×10^{-2}	1.3×10^{-5}
10	1.5×10^{-4}	1.8×10^{-2}	1.5×10^{-4}
11	1.1×10^{-4}	3.3×10^{-2}	1.1×10^{-4}
12	1.6×10^{-5}	1.6×10^{-2}	1.6×10^{-5}
13	1.0×10^{-4}	6.7×10^{-2}	1.0×10^{-4}
14	3.5×10^{-5}	2.0×10^{-2}	3.5×10^{-5}
15	4.2×10^{-5}	1.2×10^{-3}	4.3×10^{-5}
16	2.4×10^{-6}	3.4×10^{-4}	2.5×10^{-6}

Table 3- Calculated conductivity values base on the recorded electrochemical impedance spectra of each samples. σ_{total} = total conductivity, σ_g = grain conductivity and σ_{gb} = grain boundary conductivity. All the values are normalized concerning the electrode area and the thickness of the disk.

Based on the fact that the resistance of grains and grain boundaries behave like a serial circuit ($R_{total} = R_b + R_{gb}$), and taking into account the conductivity values (Table 2), it can be concluded that the rate limiting step of ion migration in this conductive system is the conduction through the grain boundaries.

The results of Table 3 reveal that samples 10 and 11 are evaluated as the two most conductive samples. Although the grain conductivity for sample 11 is higher, the ions migrate faster through grain boundaries of sample 10. Consequently, sample no. 10 is performed as the most conductive sample among all others in this study. Figure 3 shows a schematic comparison of three possible conductivity classes between these two samples .

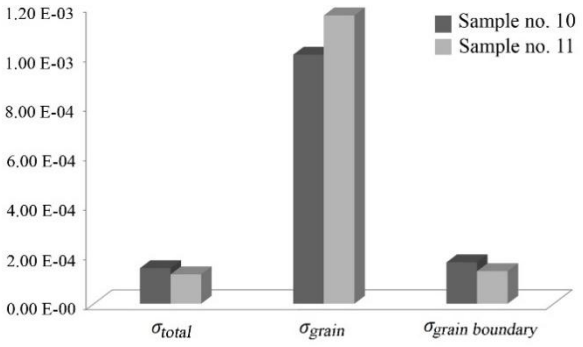

Figure 3- Schematic comparison between two most conductive samples of this study (sample no 10 and 11). Higher grain conductivity for sample no. 11 is due to the presence of larger fraction of conductive phase in the structure, however its lower grain boundary conductivity is due to the fact that this sample has lower crystallinity in compare with sample no 10.

Looking through the results of grain conductivity (σ_g) demonstrates that sample 13 is the most conductive sample. However, due to its low σ_{gb}, the final value of the overall conductivity is inconsiderable .

It can be assumed that the low grain boundary conductivity (σ_{gb}) of this sample results from the small size of the grains in this structure. To evaluate this hypothesis, the duration of the sintering process was increased from 2 to 6 h. A longer dwelling time at high temperature leads to a better diffusion and larger grains in the structure. Therefore, the proportion of grain boundaries as resistance barrier drops. This phenomenon can be observed in Figure 4, where the curvature corresponding to the sample sintered for 2 h, is almost eliminated for the sample sintered for 6 h. Overall conductivity of the samples sintered for 2 and 6 h is 1.02×10^{-4} and 1.18×10^{-3} S cm^{-1}, respectively.

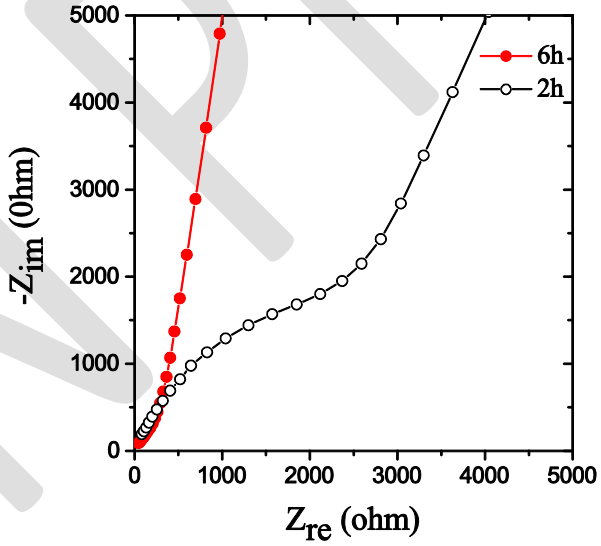

Figure 4- The effect of sintering time on the impedance behavior of Sample 13. Longer dwelling time at high temperature caused an increase in grain boundary conductivity which is a sign of courser grains of the structure.

3.2. X-Ray Diffraction Study

To have a better understanding of the difference between sample 10 and 11, the XRD patterns of these two structures were recorded (Figure 5). In order to identify the phases present in each sample, these were compared with the corresponding patterns presented in previous studies [19, 40].

The result of this comparison shows the successful synthesis of pure LATP. The pattern was easily indexed to rhombohedral unit cell ($R\bar{3}C$ space group), using Le-bail refinement with GSAS software. The lattice constant of the corresponding hexagonal cell (a, c) are determined as 8.5000(7) and 20.817(4) Å; while the reported parameters for $LiTi_2(PO_4)_3$ structure is 8.51 and 20.88 Å [41]. Small shrinkages in A and C axes are the result of Ti/Al substitution [42, 43]. While this doping leads to a decrease of the cell parameters, increasing the population of Lithium ions maintains the stability of the electrical charge balance of the system. This impregnation will enhance the conductivity of the system.

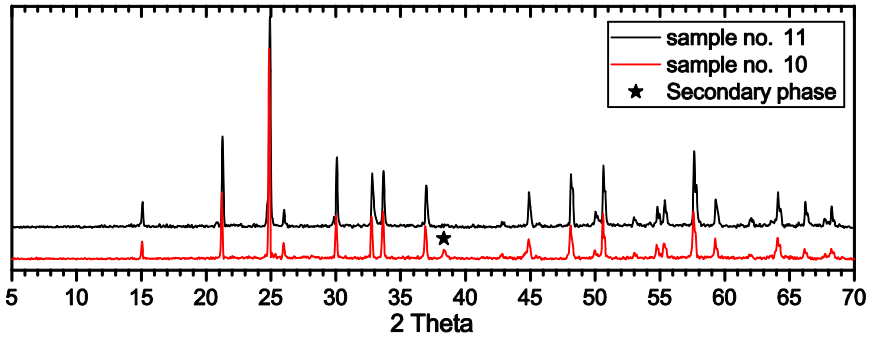

Figure 5- XRD recorded patterns (Cu-Kα) of two most conductive samples (no 10 and 11). (□) belongs to a secondary phase. Sample no.10, shows sharper peaks with larger signal to noise value. However, the recorded pattern of sample no. 11 represents broader peaks which is due to smaller size of crystallite. Shown extra peak (□) in sample no. 10 is owed to the presence of secondary phase in the structure.

Talking about the previous comparison, the full width at half maximum (FWHM) of the samples 10 and 11 were measured as 0.08 and 0.12, respectively. With respect to the inverse relationship between the grain size and FWHM, sample 10 has larger grain size as compared to sample 11. This observation is in accordance with the calculated grain boundary conductivities of EIS data.

On the other hand, a small fraction of secondary phase (□) can be seen in sample 10 (Figure 5). As a result, the conductivity of the crystalline part (σ_b) will be less than the sample 11, which contains pure NASICON structure.

3.3. The statistical analysis of the responses

The purpose of the statistical analysis of the responses (the conductivity values obtained from Electrochemical Impedance Spectroscopy) is: justifying the trend of response variation by changing the level of the factors, the importance of factors influencing the response and finally suggesting a correlation between the factors and the responses.

ANOVA and ANOM studies on the experimental data were carried out to determine the significant synthesis parameters and the optimum combination of synthesis parameters associated with σ_b, σ_{gb} and σ_{total}.

3.3.1. ANOM analysis:

The analysis of means (ANOM) is used to define the optimum combination of parameters, and estimating the main effects of the individual parameter [44]. The average values for the logarithm of σ_g, σ_{gb} and σ_{total} at levels 1, 2, 3 and 4 of the five input synthesis parameters have been considered as the main effect of the individual parameters. The main effect of the different synthesis parameters on different responses can be seen in Figure 6. The strong correlation between the total conductivity and conduction through grain boundaries can be observed in this figure for each synthesis parameter .

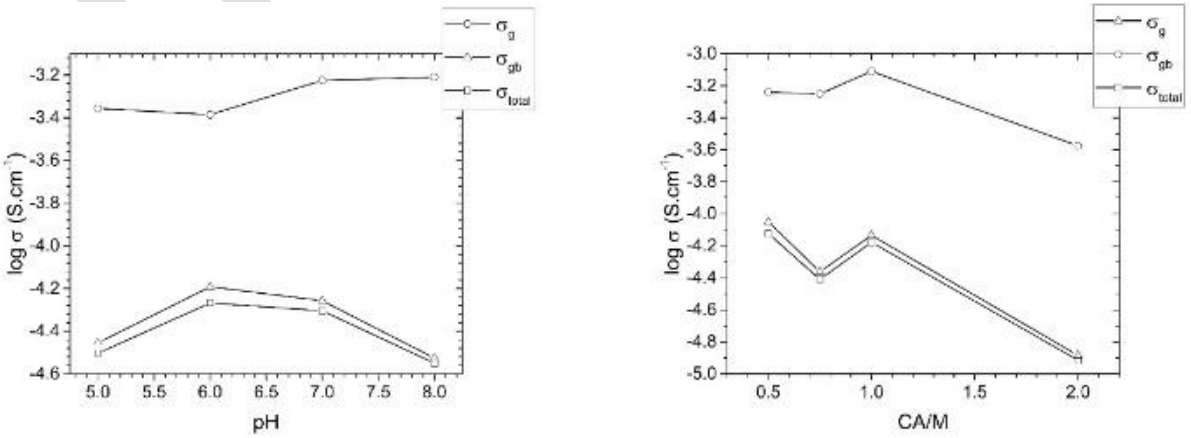

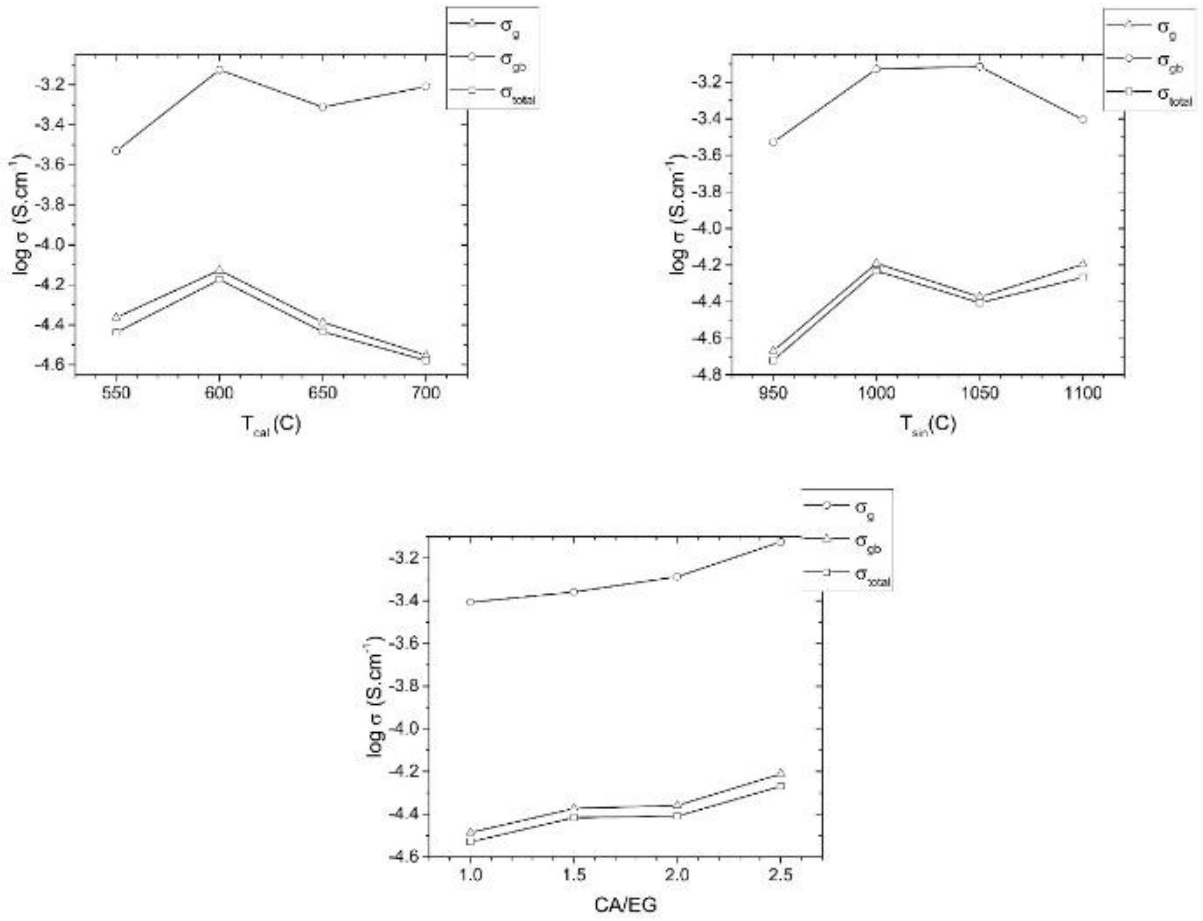

Figure 6- The main effect of each synthesis parameters on σg, σgb and σtotal. a) There is an upward trend in the case of grain conductivity while for the grain-boundary conduction the maximum value can be achieved pH=6. b) High values of citric acid increases the possibility of second phase formation and a structure with fine grains. c) Smaller amount of EG enhances the quality of the Pechini gel with final structure with courser grains. d) The best temperature for the calcination propose would be at 600°C, where larger grains LATP ceramic will forms. e) Although High sintering temperature will increase the grain growth rate, some secondary phased may forms due to the decomposition of NASICON structure.

In fact, it is not possible to infer the observed oscillation of the plotted curves, due to the complex chemistry of this system. There are some standard facts which can be used as evidence of such behavior. Further investigation requires more analysis, which is not the aim of this study. The possible hypothesizes can be listed as follows:

- The dissociation of citric acid and ethylene glycol is highly dependent on pH [45].
- An increase in the nucleation sites under high ethylene glycol concentrations [46].
- In high concentrations of citric acid, more numbers of CA molecules can chelate the metal ion. Larger complex requires diffusion in a long way in the chemical reaction to take part. It means a high probability of the formation of by-phase [46].

- The prevention of crystal growth as a result of an increase in the calcination temperature. Therefore, the higher temperature of calcination, produces smaller particle size [47].
- The decomposition of NASICON structure at high sintering temperature [48].

Here the optimum conditions for the synthesis of a structure with a maximum total conductivity can be obtained. In some cases, the mean of two different levels are almost the same, therefore, the level which causes the highest grain conductivity is selected as the optimum synthesis condition.

The optimum values for the synthesis parameters are pH: 7, CA/M: 1, CA/EG: 2.5, Tcal: 600ºC and Tsin: 1000ºC, (Figure 6).

3.3.2. ANOVA analysis:

Although ANOM (where only simple arithmetic operations are included) generates answers to major problems, the questions concerning the influence of factors on the variation of results can only be answered by analysis of variance (ANOVA). For this reason, the variance of all three responses was analyzed by this method. The contribution of each parameter can be summarized as the result of SSfactor to SStotal ratio (Figure 7).

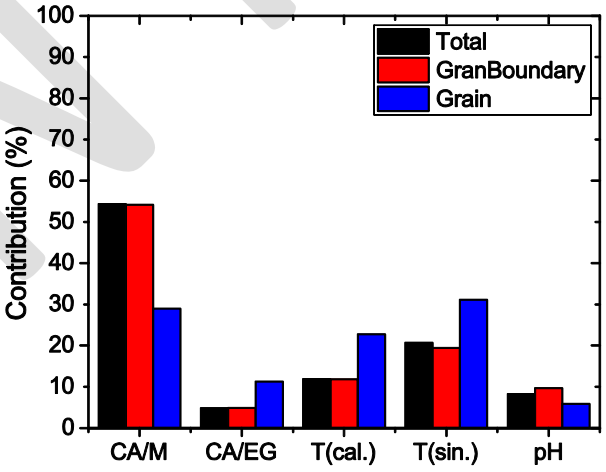

Figure 7- Contribution percentage of each selected parameter for different responses. The concentration of citric acid has been presented as the most important parameter for all the types of conductivity. While change in sintering temperature will impose larger fluctuation in case of grain conduction in compare with conductivity through grain boundaries.

3.3.3. Stepwise Regression:

The mathematical models for σg, σgb and σtotal were established by stepwise regression method. The backward elimination approach (one-sided p< 0.05) begins with the first and second order of the parameters in addition to any interaction terms .

The ability of the stepwise model to represent the experimental data is evaluated by ANOVA. The results of ANOVA for stepwise model of σ_{total} are shown in Table 4 .

Table 4- The degree of freedom value represents the number of terms in the proposed mathematical model. The small difference between the values of adjusted R square and predictable R square can confirm the goodness of the fit [49,50].

Source	DF	F-Value	P-Value	R^2 (adj)	R^2 (prd)
Grain conductivity					
Regression	5	597.69	0.000	99.47	99.2
Error	11				
Grain boundary conductivity					
Regression	3	901.95	0.000	99.41	99.2
Error	13				
Total conductivity					
Regression	3	1011.24	0.000	99.47	99.3
Error	13				

Since in these cases, P values of the regression are less than 0.05, the mathematical relationship between σ_i (I = g, gb and total) and the synthesis parameter is appropriate and the following equations are obtained as follows:

$$log\sigma_g = -1.496\, CA/M - 1.161\, CA/EG - 0.001978\, T_{sin} + 0.737\, CA/M \times CA/EG + 0.0865\, CA/EG \times pH$$

$$log\sigma_{gb} = -0.00956\, T_{sin} + 0.000006\, T_{sin} \times T_{sin} - 0.0749\, pH \times CA/M$$

$$log\sigma_{total} = -0.501\, CA/M - 0.00988\, T_{sin} + 0.000006\, T_{sin} \times T_{sin}$$

3.3.4. Interaction terms

Figure 8 presents three proposed interaction terms in the mathematical models. Although the first two terms do not show any significant interaction, the CA/EG behaves differently in altered concentrations of citric acid. The above mentioned direct correlation between lower EG concentration and grain size is effective while a sufficient amount of citric acid in the solution is available. However, lowering the amount of EG (high values of CA/EG) limits the esterification

reaction due to the lack of reactant; because there is small amount of functional groups of the citric acid to bond with ethylene glycol. Weak gelation reaction is followed by inhomogeneity in the distribution of the metal ions and less crystalized structure after sintering is obtained. This disorder has a direct influence on the conduction through grain boundaries .

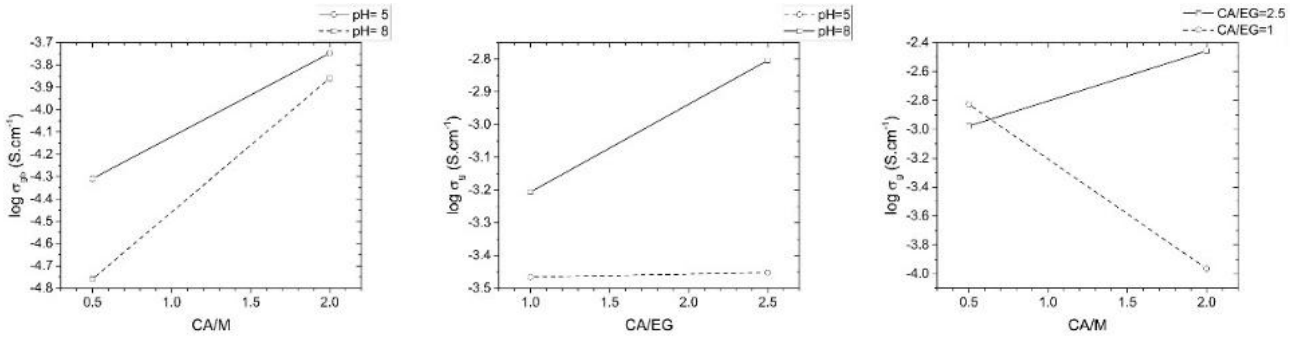

Figure 8- Interaction terms in mathematical model. a,b) pH has little impact on the function of the CA/M and CA/EG. c) Ethylene glycol behaves contrary in different concentration of citric acid in the production of LATP structure.

4. Conclusions

LATP structure $Li_{1.4}Al_{0.4}Ti_{1.6}(PO_4)_3$ was successfully synthesized by wet chemical method. In this study, peroxo-titanium precursor was used as the titanium source. Phase structure study proves the achievement of high purity NASICON phase. The electrochemical impedance spectroscopy results for some tryouts show a remarkable value of conductivity (in the order of 10^{-3} $S.cm^{-1}$). The values given for the total lithium conductions ranged from 10^{-4} $S.cm^{-1}$ [25, 51-53]. Xu et al. (2008) [40] have previously reported that the total conduction is in the same range for the same structure using SPS technique (Spark Plasma Sintering); which has its own specific complexities and intricacies. However, by using easy and convenient Pechini method the LATP structure with the maximum total conduction of 1.18×10^{-3} $S.cm^{-1}$ can be attained.

The statistics show the amount of the contribution for grain and grain boundary conductivity. In both cases, CA/M is the most influential parameter which is followed by sintering temperature as the second significant factor. The proposed mathematical formulas contain three interaction terms

in which CA/M×CA/EG has the higher coefficient than other two terms. This fact is due to the very different trend for the impact of CA/EG on the grain conductivity .

5. References:

[1] A.M. Al-Syadi, M.S. Al-Assiri, H.M.A. Hassan, M.M. El-Desoky, Grain size effects on dynamics of Li-ions in Li3V2(PO4)3 glass-ceramic nanocomposites, Ionics, 2016. 1-10.

[2] V.A. Sugiawati, F. Vacandio, M. Eyraud, P. Knauth, T. Djenizian, Porous NASICON-Type Li3Fe2(PO4)3 Thin Film Deposited by RF Sputtering as Cathode Material for Li-Ion Microbatteries, Nanoscale Research Letters, 2016, 11.

[3] S. Song, H.M. Duong, A.M. Korsunsky, N. Hu, L. Lu, A Na+ Superionic Conductor for Room-Temperature Sodium Batteries, Scientific Reports, 2016, 6.

[4] T. Zhong, F. Jiang, W. Zhao, X. Liang, Solid electrolyte potentiometric methanol gas sensor, Kuei Suan Jen Hsueh Pao/Journal of the Chinese Ceramic Society, 2016, 44, 155-158.

[5] H. Zhang, T. Zhong, R. Sun, X. Liang, G. Lu, Sub-ppm H2S sensor based on NASICON and CoCr2-xMnxO4 sensing electrode, RSC Advances, 2014, 4, 55334-55340.

[6] P. Lorenc, A. Strzelczyk, B. Chachulski, G. Jasinski, Properties of Nasicon-based CO2 sensors with Bi8Nb2O17 reference electrode, Solid State Ionics, 2015, 271, 48-55.

[7] K.M. Hercule, Q. Wei, O.K. Asare, L. Qu, A.M. Khan, M. Yan, C. Du, W. Chen, L. Mai, Interconnected nanorods-nanoflakes Li2Co2(MoO4)3 framework structure with enhanced electrochemical properties for supercapacitors, Advanced Energy Materials, 2015, 5.

[8] N. Gorodylova, V. Kosinová, Ž. Dohnalová, P. Šulcová, P. Bělina, Thermal stability and colour properties of CuZr4(PO4)6, Journal of Thermal Analysis and Calorimetry, 2016, 1-8.

[9] Y. Shimizu, T. Ushijima, Sol-gel processing of NASICON thin film using aqueous complex precursor, Solid State Ionics, 2000, 132, 143-148.

[10] R. Klee, P. Lavela, M.J. Aragón, R. Alcántara, J.L. Tirado, Enhanced high-rate performance of manganese substituted Na3V2(PO4)3/C as cathode for sodium-ion batteries, Journal of Power Sources, 2016, 313, 73-80.

[11] S. Kumar, P. Balaya, Improved ionic conductivity in NASICON-type Sr2 + doped LiZr2(PO4)3, Solid State Ionics, 2016, 296, 1-6.

[12] F. Ma, E. Zhao, S. Zhu, W. Yan, D. Sun, Y. Jin, C. Nan, Preparation and evaluation of high lithium ion conductivity Li1.3Al0.3Ti1.7(PO4)3 solid electrolyte obtained using a new solution method, Solid State Ionics, 2016, 295, 7-12.

[13] S. Kim, V. Mathew, J. Kang, J. Gim, J. Song, J. Jo, J. Kim, High rate capability of LiFePO4 cathodes doped with a high amount of Ti, Ceramics International, 2016, 42, 7230-7236.

[14] D.H. Kothari, D.K. Kanchan, Effect of doping of trivalent cations Ga3+, Sc3+, Y3+ in Li1.3Al0.3Ti1.7 (PO4)3 (LATP) system on Li+ ion conductivity, Physica B: Condensed Matter, 2016, 501, 90-94.

[15] D.H. Kothari, D.K. Kanchan, Study of Li+ conduction in Li1.3Al0.3-xScxTi1.7(PO4)3 (x=0.01, 0.03, 0.05 and 0.07) NASICON ceramic compound, Physica B: Condensed Matter, 2016, 494, 20-25.

[16] M.Y. Hassaan, Z. Kaixin, J. Wang, M.G. Moustafa, Mössbauer and electrical conduction investigations of LiFe(BaTi)(PO4) NASICON nano composite, Hyperfine Interactions, 2016, 237, 1-15.

[17] M.Y. Hassaan, S.M. Salem, M.G. Moustafa, S. Kubuki, K. Matsuda, T. Nishida, Controlled crystallization a ionic conductivity of nanostructured LiNbFePO4 glass ceramic, Hyperfine Interactions, 2014, 226, 131-140.

[18] M. Illbeigi, A. Fazlali, M. Kazazi, A.H. Mohammadi, Effect of simultaneous addition of aluminum and chromium on the lithium ionic conductivity of LiGe2(PO4)3 NASICON-type glass-ceramics, Solid State Ionics, 2016, 289, 180-187.

[19] X. Xu, Z. Wen, J. Wu, X. Yang, Preparation and electrical properties of NASICON-type structured Li1.4Al0.4Ti1.6(PO4)3 glass-ceramics by the citric acid-assisted sol-gel method, Solid State Ionics, 2007, 178, 29-34.

[20] K. Dokko, K. Hoshina, H. Nakano, K. Kanamura, Preparation of LiMn2O4 thin-film electrode on Li1+xAlxTi2-x(PO4)3 NASICON-type solid electrolyte, Journal of Power Sources, 2007, 174, 1100-1103.

[21] E. Christensen, J.H. Von Barner, J. Engell, N.J. Bjerrum, Preparation of CuZr2P3O12 from alkoxide-derived gels: phase formation as a function of heat treatment, Journal of Materials Science, 1990, 25, 4060-4065.

[22] N.S. Bell, C. Edney, J.S. Wheeler, D. Ingersoll, E.D. Spoerke, The influences of excess sodium on low-temperature NaSICON synthesis, Journal of the American Ceramic Society, 2014, 97, 3744-3748.

[23] F. Ejehi, S.P.H. Marashi, M.R. Ghaani, D.F. Haghshenas, The synthesis of NaSICON-type ZrNb(PO4) 3 structure by the use of Pechini method, Ceramics International, 2012, 38, 6857-6863.

[24] V. Aravindan, M. Ulaganathan, W.C. Ling, S. Madhavi, Fabrication of New 2.4V Lithium-Ion Cell with Carbon-Coated LiTi2(PO4)3 as the Cathode, ChemElectroChem, 2015, 2, 231-235.

[25] E. Zhao, F. Ma, Y. Jin, K. Kanamura, Pechini synthesis of high ionic conductivity Li1.3Al0.3Ti1.7 (PO4)3 solid electrolytes: The effect of dispersant, Journal of Alloys and Compounds, 2016, 680, 646-653.

[26] C.R. Mariappan, C. Galven, M.P. Crosnier-Lopez, F. Le Berre, O. Bohnke, Synthesis of nanostructured LiTi2(PO4)3 powder by a Pechini-type polymerizable complex method, Journal of Solid State Chemistry, 2006, 179, 450-456.

[27] M.A. Gomes, Á.S. Lima, K.I.B. Eguiluz, G.R. Salazar-Banda, Wet chemical synthesis of rare earth-doped barium titanate nanoparticles, Journal of Materials Science, 2016, 51, 4709-4727.

[28] D. Segal, Chemical synthesis of ceramic materials, Journal of Materials Chemistry, 1997, 7, 1297-1305.

[29] A. Akrami, A. Niazi, Synthesis of maghemite nanoparticles and its application for removal of Titan yellow from aqueous solutions using full factorial design, Desalination and Water Treatment, 2016, 57, 22618-22631.

[30] S.J. Park, H.K. An, Optimization of fabrication parameters for nanofibrous composite membrane using response surface methodology, Desalination and Water Treatment, 2016, 57, 20188-20198.

[31] B.A.E. Ben-Arfa, I.M.M. Salvado, J.R. Frade, R.C. Pullar, Fast route for synthesis of stoichiometric hydroxyapatite by employing the Taguchi method, Materials and Design, 2016, 109, 547-555.

[32] H. Toshiyoshi, T. Konishi, K. Machida, K. Masu, A mixed-design technique for integrated MEMS using a circuit simulator with HDL, Proceedings of the 20th International Conference on Mixed Design of Integrated Circuits and Systems, MIXDES 2013, 2013, pp. 17-22.

[33] M. Natsume, J.H. Kim, S. Yonezawa, M. Takashima, Preparation and characterization of nano-sized BaTiO3 particles using aqueous peroxotitanium acid solution: Effects of pH adjustment, Materials Chemistry and Physics, 2014, 148, 169-174.

[34] M. Hajizadeh-Oghaz, R. Shoja Razavi, M. Khajelakzay, Optimizing sol–gel synthesis of magnesia-stabilized zirconia (MSZ) nanoparticles using Taguchi robust design for thermal barrier coatings (TBCs) applications, Journal of Sol-Gel Science and Technology, 2014, 73, 227-241.

[35] R. Roy, Design Of Experiment using the Taguchi approach, Wiley Interscience 2001.

[36] C.R. Gautam, D. Kumar, P. Singh, O. Parkash, Study of Impedance Spectroscopy of Ferroelectric (Pb Sr)TiO3 Glass Ceramic System with Addition of La2O3, ISRN Spectroscopy, 2012, 11.

[37] J.-S. Lee, C.-M. Chang, Y.I.L. Lee, J.-H. Lee, S.-H. Hong, Spark Plasma Sintering (SPS) of NASICON Ceramics, Journal of the American Ceramic Society, 2004, 87, 305-307.

[38] A. Ahmad, T.A. Wheat, A.K. Kuriakose, J.D. Canaday, A.G. McDonald, Dependence of the properties of Nasicons on their composition and processing, Solid State Ionics, 1987, 24, 89-97.

[39] Y. Noguchi, E. Kobayashi, L.S. Plashnitsa, S. Okada, J.-i. Yamaki, Fabrication and performances of all solid-state symmetric sodium battery based on NASICON-related compounds, Electrochimica Acta, 2013, 101 59-65.

[40] X. Xu, Z. Wen, X. Yang, L. Chen, Dense nanostructured solid electrolyte with high Li-ion conductivity by spark plasma sintering technique, Materials Research Bulletin, 2008, 43, 2334-2341.

[41] E. Kazakevicius, A. Urcinskas, A. Kezionis, A. Dindune, Z. Kanepe, J. Ronis, Electrical properties of Li1.3Ge1.4Ti0.3Al0.3(PO4)3 superionic ceramics, Electrochimica Acta, 2006, 51, 6199-6202.

[42] K. Arbi, M.G. Lazarraga, D. Ben Hassen Chehimi, M. Ayadi-Trabelsi, J.M. Rojo, J. Sanz, Lithium Mobility in Li1.2Ti1.8R0.2(PO4)3 Compounds (R = Al, Ga, Sc, In) as Followed by NMR and Impedance Spectroscopy, Chemistry of Materials, 2003, 16, 255-262.

[43] K. Arbi, J.M. Rojo, J. Sanz, Lithium mobility in titanium based Nasicon Li1+xTi2-xAlx(PO4)3 and LiTi2-x Zrx(PO4)3 materials followed by NMR and impedance spectroscopy, Journal of the European Ceramic Society, 2007, 27, 4215-4218.

[44] M.S. Phadke, Quality Engineering Using Robust Design, Prentice Hall, 1989.

[45] D.L. Tran, Q.Q. Ngo, Cathode materials for rechargeable Li-ion batteries: Sol-Gel synthesis and characterization of LiMn2O4 and LiCuxMn2-xO4 ,2004

[46] S.G. Rudisill, N.M. Hein, D. Terzic, A. Stein, Controlling Microstructural Evolution in Pechini Gels through the Interplay between Precursor Complexation, Step-Growth Polymerization, and Template Confinement, Chemistry of Materials, 2013, 25, 745-753.

[47] F. Acosta-Humánez, O. Almanza, C. Vargas-Hernández, Effect of sintering temperature on the structure and mean crystallite size of Zn1-xCoxO (x = 0.01 - 0.05) samples, Superficies y Vacio, 2014. 27, 43-48.

[48] Q. Ma, M. Guin, S. Naqash, C.-L. Tsai, F. Tietz, O. Guillon, Scandium-Substituted Na3Zr2(SiO4)2(PO4) Prepared by a Solution-Assisted Solid-State Reaction Method as Sodium-Ion Conductors, Chemistry of Materials, 2016, 28. 4821-4828.

[49] I.S. Fahim, S.M. Elhaggar, H. Elayat, Experimental Investigation of Natural Fiber Reinforced Polymers, Materials Sciences and Applications, 2012, 03, 4.

[50] A.M. Alshaibani, Z. Yaakob, A.M. Alsobaai, M. Sahri, Optimization of Pd-B/³-Al2O3 catalyst preparation for palm oil hydrogenation by response surface methodology (RSM), Brazilian Journal of Chemical Engineering, 2014, 31, 69-78.

[51] C. Davis, J.C. Nino, Microwave Processing for Improved Ionic Conductivity in Li2O-Al2O3-TiO2-P2O5 Glass-Ceramics, Journal of the American Ceramic Society, 2015, 98, 2422-2427.

[52] K. Arbi, W. Bucheli, R. Jiménez, J. Sanz, High lithium ion conducting solid electrolytes based on NASICON Li1+xAlxM2-x(PO4)3 materials (M = Ti, Ge and $0 \leq x \leq 0.5$), Journal of the European Ceramic Society, 2015, 35, 1477-1484.

[53] K. Waetzig, A. Rost, U. Langklotz, B. Matthey, J. Schilm, An explanation of the microcrack formation in Li1.3Al0.3Ti1.7(PO4)3 ceramics, Journal of the European Ceramic Society, 2016, 36, 1995-2001